Evaluation of the effect of two Naproxen-Based Hydrazones on the corrosion inhibition of Mild Steel in 1.0 M HCl

Maryam Chafiq[1], Abdelkarim Chaouiki [1], Mustafa R. Al-Hadeethi [2], Hassane Lgaz [3,], Rachid Salghi [1], Siham K. AbdelRaheem[4], Ismat H. Ali [4], Sara A. M. Ebraheem[4], Shaaban K. Mohamed [5,6], Ill-Min Chung[3,*]*

[1]Laboratory of Applied Chemistry and Environment, ENSA, University Ibn Zohr, PO Box 1136, Agadir, Morocco;
[2]College of Education, Department of Chemistry, Kirkuk University, Kirkuk, Iraq;
[3]Department of Crop Science, College of Sanghur Life Science, Konkuk University, Seoul 05029, South Korea
[4]Department of Chemistry, College of Science, King Khalid University, P. O. Box 9004, Postal Code 61413, Abha, Kingdom of Saudi Arabia;
[5]Chemistry and Environmental Division, Manchester Metropolitan University, Manchester, United Kingdom;
[6]Chemistry Department, Faculty of Science, Minia University, El-Minia, Egypt;
[*]E-mail: hlgaz@konkuk.ac.kr (H. L.), imcim@konkuk.ac.kr (I-M. C.)

During the past years, there has been an increasingly important emphasis on the study of corrosion inhibitors because of their performance in inhibiting the dissolution of metals in various corrosive mediums, making research into the use of environmentally safer substances a goal for corrosion scientists. On this wise, the anti-corrosive performance of (E)-N'-(4-chlorobenzylidene)-2-(6-methoxynaphthalen-2-yl) propanehydrazide (CBMP) and ((E)-2-(6-methoxynaphthalen-2-yl)-N'-(4-methylbenzylidene) propanehydrazide (MMBH) for mild steel (MS) in 1.0 M HCl has been studied employing electrochemical methods, weight loss and SEM/EDX examinations. An increase in the concentration of the inhibitor up to an optimized level of 5×10^{-3} M has significantly improved the corrosion rate (i_{corr}) values. The preferential protective response of MMBH against corrosion has been investigated in a range of temperature settings of 303 K-333 K. It is strongly implied by the results of the PDP experiments that the selected inhibitors acted as mixed-type inhibitors with a more pronounced cathodic nature. The adsorption of both compounds follows the Langmuir isotherm. SEM/EDX confirmed the good inhibition performance of tested compounds.

Keywords: Corrosion inhibition; Mild steel; SEM/EDX; Electrochemical measurements.

1. INTRODUCTION

In the industrial sector, acid solutions find extensive usage in the pickling or cleaning with acid as well as on the elimination of all kinds of localized deposits caused by rust [1]. At the same time, many industrial treatments necessitate the introduction of acid solutions in one or more stages of production. One of these is hydrochloric acid, which is very often used [2,3]. On the other hand, the most common type of metal encountered throughout these industries is mild steel because of its mechanical advantages, ultimate thermal stability, high tensile strength, and affordability. Inevitably, these kinds of processes, disastrously, put metallic materials at risk, causing their acidic corrosion. Corrodible installations and industrial equipment prone to corrosion have been carefully intended taking into consideration the attainable anti-corrosion protection approaches. Some corrosion protectors which have been successfully deployed in the area of metal conservation are suitable for industrial applications [4–8]. One such method concerns the utilization of inhibitors which have now become widely used as they are considered being the safest, the strongest and economically they are the most inexpensive solution against the aggressive effects of metals corrosion [9–14]. Concern for boosting the benefits of green products in terms of performance enhancement has turned into an exciting and challenging endeavor for chemists and technologists around the world. Against this background, two new compounds have been developed to improve the anti-corrosion effect of two new compounds, which are (E)-N'-(4-chlorobenzylidene)-2-(6-methoxynaphthalen-2-yl) propanehydrazide (CBMP) and ((E)-2-(6-methoxynaphthalen-2-yl)-N'-(4-methylbenzylidene) propanehydrazide (MMBH) for MS in the 1.0 M HCl solution. The combination of aromatic rings, oxygen and nitrogen atoms, which are the source of electrons capable of promoting the adsorption of the two molecules being tested on the surface of the MS, has been the main basis for the choice of these molecules. As such, Hydrazones contain azomethine group R1R2-C=NNH2 where R1 and R2 are different functional groups so that hydrazones are very important starting materials in bioactive heterocycles [15]. On the other hand, Naproxen has been considered as the most effective Non-steroidal Anti-inflammatory Drugs (NSAIDs) since long, but because of its carboxylic group, there were some limitations. To minimize the side effects and to enhance the anti-inflammatory activity, the functionalization of the carboxylic group is a key step [16]. One of the most effective functionalization of the carboxylic group is its conversion into hydrazone derivatives [17]. Nowadays, many trial studies have been conducted to develop corrosion inhibitors based on hydrazones derived from NSAIDs to protect a broad range of metals and alloys [18–20].

For this work, our focus was on the synthesis and electrochemical study of new naproxen-based hydrazones that are anticipated to inhibit the corrosion of steel in an acidic medium. Electrochemical Impedance Spectroscopy (EIS), Weight loss measures (WL), as well as Potentiodynamic Polarization (PDP), are selected as experimental methods to check the resistance of MS in the presence of the CBMP and MMBH in the studied medium. Using gravimetric measurements, temperatures were varied from 303K to 333K to look at the response of temperature to the efficiency of MMBH. Further, the effect of immersion time was monitored by the EIS method for 24 hours in the optimum temperature. To provide further interpretation of the data, an area analysis using SEM/EDX method was conducted.

2. MATERIAL AND METHODS

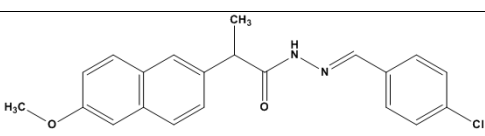### 2.1. Solution, metal sample preparation and inhibitors

Tests have been conducted on MS samples, the chemical composition (%) of which is shown in Table 1.

Table 1. Chemical composition of the studied MS.

Atom	Content (%)
Fe	98.388
C	0.371
Si	0.229
Mn	0.681
S	0.014
Cr	0.076
Ti	0.012
Ni	0.058
Co	0.010
Cu	0.161

The electrolyte is a solution prepared from a 37% HCl solution of the brand Sigma-Aldrich which was used to prepare 1.0 M HCl aggressive control solution by diluting it with distilled water. Using a rotating disc containing 400, 800, 1200 and 1600 grit emery papers, the samples of mild steel were smoothed with the polishing machine before each test. Following this, acetone degrease was applied to the MS samples; they were rinsed with distilled water, followed by drying of the sample under a draught. In an interval of concentration from 1×10^{-4} M to 5×10^{-3} M, the anti-corrosion effect of CBMP and MMBH has been analyzed on mild steel (MS). Table 2 describes inhibitors molecular structures under test along with their characterization. The full synthesis procedure is described in details in our recent paper [21].

Table 2. Molecular structures of MMBH and CBMP along with their characterization.

Inhibitors	Names and abbreviation
	(E)-N'-(4-chlorobenzylidene)-2-(6-methoxynaphthalen-2-yl)propanehydrazide (CBMP) m.p=157-160 ^{0}C. IR (KBr): (C=O amide 1662 cm^{-1}), (N-H 3197 cm^{-1}), (-C=N 1614 cm^{-1}). ^{1}H NMR (400MHz, DMSO): δ = 1.4 (d, 3H, CH$_3$), 3.5 (q, 1H, C-H), 3.8 (s, 3H, OCH$_3$), 8.2 (s, 1H, -CH=N-), 10.3 (s, 1H, -NH), 7.1-8.0 (m, 10H, aromatic protons). ^{13}C-NMR δ =18 (CH$_3$), 44 (C-H aliphatic), 55 (OCH$_3$), 107-156 (16 aromatic carbons), 162 (C=N), 165 (C=O amide).
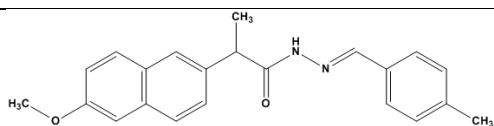
(E)-2-(6-methoxynaphthalen-2-yl)-N'-(4-methylbenzylidene) propanehydrazide (MMBH)

m.p=190-193 ^{0}C. IR (KBr): (C=O amide 1655 cm^{-1}), (N-H 3236 cm^{-1}), (-C=N 1610 cm^{-1}). ^{1}H NMR (400MHz, DMSO): δ = 1.4 (d, 3H, CH$_3$), 2.3 (s, 3H, CH$_3$), 3.5 (q, 1H, C-H), 3.8 (s, 3H, OCH$_3$), 8.3 (s, 1H, -CH=N-), 10.5 (s, 1H,-NH), 7.1-8.0 (m, 10H, aromatic protons). ^{13}C-NMR δ =18 (CH$_3$), 44 (C-H aliphatic), 55 (OCH$_3$), 107-155 (16 aromatic carbons), 163 (C=N), 174 (C=O amide).

2.2. Gravimetric study

The density of the corrosion current, based on the gravimetric method, is determined in a first place for several concentrations of inhibitors and then by setting the concentration at 5×10^{-3} M the effect of the immersion time is tested. To carry out the gravimetric measurements, tests were carried out on MS in the form of rectangular pieces with a diameter of 2.3 cm x 1.9 cm and a thickness of 0.4 cm, which have been left in the inhibited solutions with tested concentrations of each molecule and in the blank for a period of 24 hours. The surface of the mild steel has been polished by using various grades of emery paper from 400 to 1600 and cleaned thoroughly. All tests have been performed as described in our previous works at a temperature range of 303-333K [18–20]. In the calculation of the corrosion rate, the difference between the final average mass and the initial mass is taken and employed in the equation (1)[22]:

$$C_{WL} = \frac{K \times W}{A \times t \times \rho} \tag{1}$$

For more information from the standard methods ASTM [23]: W referred to in the equation, means the loss in mass given in units of grams, where t indicates the immersion time, generally given in hrs and A is the exposed area in cm^2. K $= 8.76 \times 10^4$ was used as constant.

Equations 2 and 3 have been applied when calculating the inhibitory efficacy of the tested molecules and their surface coverage, respectively.

$$\eta_{WL}(\%) = \left[1 - \frac{C_{WL}}{C^{\circ}_{WL}}\right] \times 100 \tag{2}$$

$$\theta = \frac{C^{\circ}_{WL} - C_{WL}}{C^{\circ}_{WL}} \tag{3}$$

Here θ means the degree of surface coverage of CBMP and MMBH, C_{WL} and C°_{WL} refer to the corrosion rates at their studied concentrations and in 1.0 M HCl.

2.3. Electrochemical measurements

A 3-electrode cell connected to a PGZ 100 Potentiostat controlled by a "Voltalab Master 4" analysis software was used for the electrochemical tests. A saturated calomel electrode is used as the reference electrode. The auxiliary electrode is a platinum grid, and the working electrode is a mild steel electrode with a surface area of $1cm^2$ placed close to the reference electrode. At a temperature fixed at 303 ± 2 K, the electrochemical measurements are all carried out after 30 min, which was the needed time to attain a stable open circuit potential. Wherein the values of the results given for all methods are the average of three tests carried out under the same conditions for each concentration. A potential range of -800 to -200 mV with a sweep rate of 1 mV s^{-1} were used for potentiodynamic measurements. Electrochemical impedance is measured by monitoring the response of the electrochemical system to low amplitude alternating signal disturbance voltage of 5 mV in the frequency range from 10 mHz to 100 kHz.

2.4. SEM/EDX studies

The specimens' surface characterization has been performed, conducting a scanning electron microscope in combination with the analyzer, in the absence and presence of inhibitors. This was done on samples exposed for 24 hours in the corrosive environment and subjected to the pre-treatment already mentioned in the gravimetric assays. In addition, the layers formed on the treated steel coupons are identified and compared, using an EDX analyzer adapted to the SEM.

3. RESULTS AND DISCUSSION

3.1. Weight loss measurement

3.1.1. Concentration effect

An initial analytical approach regarding the anti-corrosion properties related to the MS in the acidic solution was provided by weight loss studies to evaluate the inhibitory efficacy at a constant temperature of CBMP and MMBH at different concentrations during 24 hours of immersion. Values for corrosion rate and percent inhibiting efficiency calculated gravimetrically for various concentrations of CBMP and MMBH compounds in 1.0 M HCl at 25°C are shown in Fig. 1.

Looking at Fig. 1 showed that, firstly, the corrosion rate decreases, and secondly, the inhibitory effectiveness improves with the concentration of CBMP and MMBH inhibitors, attaining a higher value of 93.14% in the presence of 5×10^{-3} M of MMBH. It proves its high efficiency as opposed to the corrosion of MS in the 1.0 M HCl environment. In comparison to CBMP, MMBH is more effective.
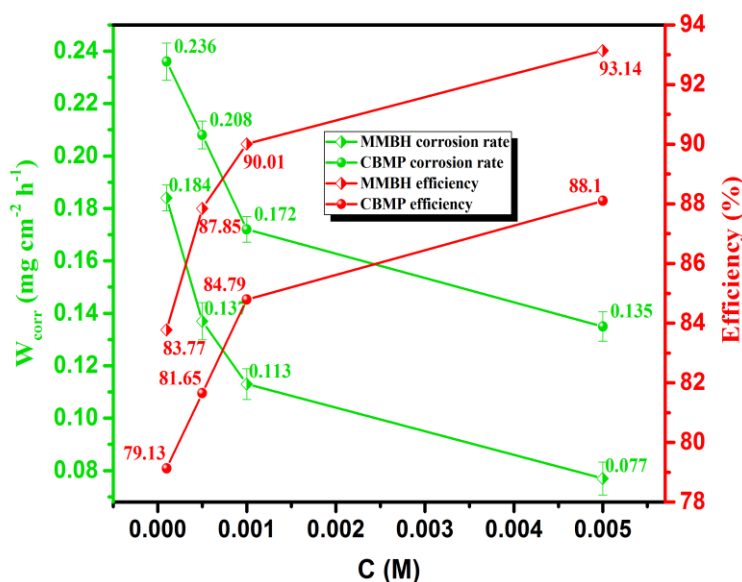
Figure 1. The relationship among corrosion rate, inhibition efficiency, and inhibitors concentrations for mild steel in 1.0 M HCl with MMBH and CBMP at 303K.

It's important as well to mention that the enhance in inhibitory efficacy with concentration is primarily dependent on the strength with which these inhibitors interact with metal surfaces, due to the heteroatoms found on the two inhibitor molecules, as well as the length of the carbon chain, especially the electronic properties of CH_3 and Cl which differentiate the inhibitory efficacy of the two studied inhibitors [24]. Moreover, these inhibitors adsorb significantly more easily on the MS that causes the development of a preventive layer that decreases the reactivity of the MS [25–27].

3.1.2. Temperature effect

The temperature control of the corrosion kinetic process may give some further information on the electrochemical behavior under aggressive conditions. We examined the thermal inhibitory mechanism of MMBH by examining the effect of temperature on the progression of corrosion rate and inhibitory efficacy over a temperature range of 303K- 333K. In the absence and presence of MMBH, the influence of temperature is summarized in Table 3.

Table 3. The temperature effect toward inhibition efficiency and corrosion rate of MMBH.

Solution		Temperature	Corrosion rate	Inhibition efficiency
		K	mg/cm^2×h	%
Blank	1.0 M HCl	303	1.1350 ± 0.0121	-
		313	1.4162 ± 0.0215	-
		323	1.9981 ± 0.0214	-
		333	2.5392 ± 0.0316	-

|				
MMBH	5×10^{-3} M	303	0.077 ± 0.0057	93.14
		313	0.110 ± 0.0097	92.21
		323	0.182 ± 0.0088	90.89
		333	0.253 ± 0.0041	90.03
	1×10^{-3} M	303	0.113 ± 0.0082	90.01
		313	0.152 ± 0.0056	89.21
		323	0.277 ± 0.0069	88.54
		333	0.345 ± 0.0076	86.38
	5×10^{-4} M	303	0.137 ± 0.0102	87.85
		313	0.201 ± 0.0029	85.79
		323	0.316 ± 0.0018	84.15
		333	0.434 ± 0.0066	82.89
	1×10^{-4} M	303	0.184 ± 0.0097	83.77
		313	0.256 ± 0.0079	81.27
		323	0.396 ± 0.0077	80.17
		333	0.517 ± 0.0034	79.63

Well, given the increase in temperature, the surface has the highest corrosion rate values. Besides, the computations of the thermodynamic parameters are done based on results of the gravity experiments to obtain an image of the observed inhibitor in HCl medium. The variation of the logarithm of the corrosion rate as a function of the inverse of the absolute temperature (Equation 4) allows getting the activation energy, while formula 5 represents the transition state equation:

$$C_{WL} = K \times e^{\frac{-E_a}{RT}} \qquad (4)$$

$$C_{WL} = \frac{RT}{Nh} \exp\left(\frac{\Delta S_a}{R}\right) \exp\left(\frac{\Delta H_a}{RT}\right) \qquad (5)$$

Here, T is the temperature of the medium, N denotes the number of Avogadro, R is the universal gas constant (8.314 J mol^{-1} K^{-1}), and h is Planck's constant.

In Fig. 2, the Arrhenius and transition state plots are depicted, which relate the logarithm of corrosion rate as a function of the inverse of the relative temperature and ln C_{WL}/T as a function of $1/T$ with and without the inhibitor. The thermodynamic parameters were estimated from the slope and intercept obtained from the curves, and the outcomes are noted in Table 4. The addition of both compounds to the 1.0 M HCl acid solution causes an increase in the value of the activation energy compared to that of the acid solution alone. This increase is shown more and more when the inhibitor is added in higher concentrations, which is often interpreted as an indication of the formation of a protective adsorption barrier on the surface by a physical and chemical mechanism. Besides, positive enthalpy values imply the endothermic nature of the MS dissolution process [24].
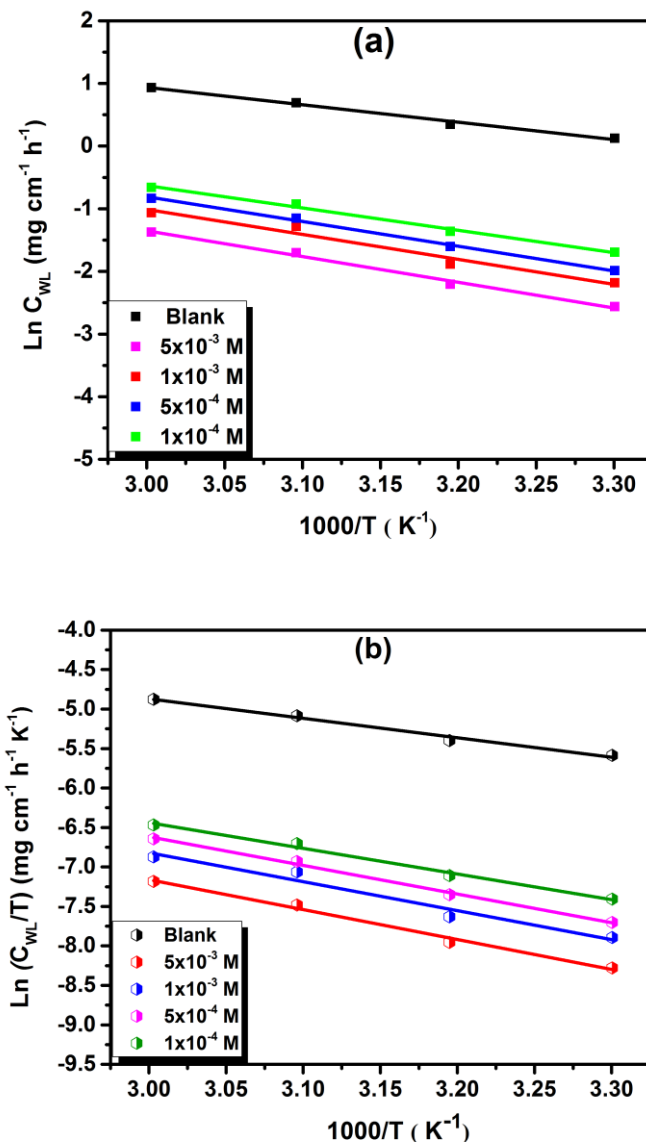
Figure 2. Arrhenius (a) and transition state (b) plots for corrosion inhibition of mild steel in the absence and presence of different concentrations of inhibitors in 1.0 M HCl.

**Table 4.** Corrosion kinetic parameters for mild steel in 1.0 M HCl in the presence and absence of MMBH.

Parameters	Blank	MMBH			
		5×10^{-3} M	1×10^{-3} M	5×10^{-4} M	1×10^{-4} M
E_a (kJ mol^{-1})	23.12	34.15	33.14	32.82	29.67
ΔH_a (kJ mol^{-1})	20.48	31.51	30.50	30.18	27.03
ΔS_a (J mol^{-1}K^{-1})	-176.48	-162.44	-162.64	-161.90	-169.88
E_a - ΔH_a (kJ mol^{-1})	2.64	2.64	2.64	2.64	2.64

Concerning ΔS_a value, it could be observed that the ΔS_a is superior to that of the uninhibited solution, and it is negative. This concludes that a fall into the disorder has occurred at the level of activated complex reaction reagents [28].

3.2. PDP study

To appraise further the corrosion inhibition characteristics obtained by interpreting the kinetics of the anodic and cathodic reactions of the corrosion process, potentiodynamic polarization (PDP) was studied in detail. After 30 min immersion of the MS in the acid solution, potentiodynamic polarization (PDP) curves obtained at different concentrations and results are presented in Fig. 3 [29].
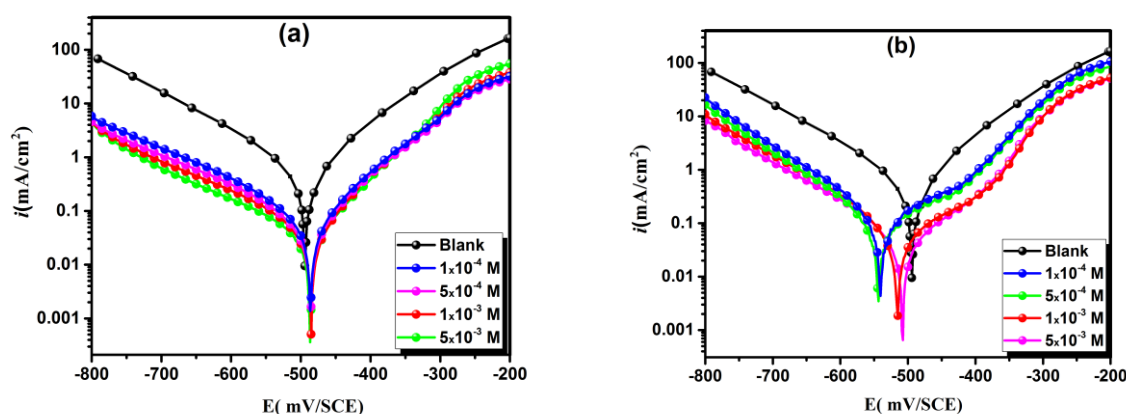
Figure 3. PDP curves of MS in hydrochloric acid solution in the presence and absence of various concentrations of MMBH (a) and CBMP (b) at 303 K

The corrosion properties of the studied systems in terms of corrosion potential, corrosion current density and Tafel slopes are determined and tabulated in Table 5. The corresponding inhibition efficiency was estimated from the current density according to equation (6):

$$\eta_{PDP}(\%) = \frac{i^{\circ}_{corr} - i_{corr}}{i^{\circ}_{corr}} \times 100 \qquad (6)$$

Where i°_{corr} and i_{corr} represent respectively, the corrosion current density of the corrosion reference solution and those of the inhibitors with different concentrations.

Adding CBMP and MMBH compounds leads to a decrease in cathodic and anodic current densities with a wide range of linearity, which is indicative that Tafel's law is adequately satisfied [30]. Note from these polarization curves that the occurrence of log i = f (E) at all concentrations is essentially the same for the two studied inhibitors, suggesting the immutable mechanism of the corrosion process [31]. In other words, these inhibitors adsorbed on the surface retarded the development of cathodic hydrogen and stopped the active dissolution of the anodic metal without changing the dissolution mechanism, as is characteristic of mixed type inhibitors [29]. As well, the inhibiting efficacy values presented in Table 5, reaches a value of 95.37% for MMBH, and 89.20% is

obtained for the 5×10^{-3} M of CBMP test. Accordingly, it can be concluded that hydrazone derivatives are potentially resistant to corrosion in the HCl medium.

Table 5. Electrochemical parameter values estimated according to PDP curves of MS in hydrochloric acid solution in the presence and absence of various concentrations of MMBH and CBMP at 303 K

| Inhibitor	Concentration (M)	$-E_{corr}$ (mV vs. SCE)	$-\beta_c$ (mV dec^{-1})	i_{corr} (mA cm^{-2})	η_{PDP} (%)
Blank	1.0	496 ± 0.4	162 ± 4.1	0.5640 ± 0.0023	-
MMBH	5×10^{-3}	489 ± 0.8	177 ± 5.9	0.0379 ± 0.0048	93.28
	1×10^{-3}	487 ± 0.7	183 ± 7.2	0.0573 ± 0.0059	89.84
	5×10^{-4}	488 ± 1.1	186 ± 2.9	0.0780 ± 0.0041	86.17
	1×10^{-4}	473 ± 0.6	138 ± 8.8	0.0968 ± 0.0063	82.83
CBMP	5×10^{-3}	510 ± 0.2	146 ± 7.4	0.0679 ± 0.0066	87.96
	1×10^{-3}	517 ± 1.6	139 ± 4.5	0.0886 ± 0.0019	84.29
	5×10^{-4}	542 ± 0.9	119 ± 5.6	0.1038 ± 0.0086	81.59
	1×10^{-4}	519 ± 1.2	124 ± 7.1	0.1215 ± 0.0046	78.45

3.3. EIS study

3.3.1. Concentration effect

The EIS studies have been performed as a means of corroborating findings derived from the polarization curve and acquiring additional knowledge on corrosion mechanisms. The Fig. 5 illustrates both Nyquist diagrams (a, b) and Bode representation (c, d) of the metal, in HCl medium, in the presence of MMBH and CBMP inhibitors at various concentrations and the blank. For each case, the double-layer electrical capacity (C_{dl}) was calculated based on the following equation:

$$C_{dl} = \sqrt[n]{Q \times R_p^{1-n}} \qquad (7)$$

With n indicating as always the phase shift, which allows calculating the surface heterogeneity of mild steel [32,33]. Based on the EIS technique, for the determination of inhibitory efficacy, the following formula is used:

$$\eta_{EIS}(\%) = \frac{R_p^i - R_p^{\circ}}{R_p^i} \times 100 \qquad (8)$$

Where R_p° and R_p^i signify the polarization resistance in the blank and with the addition of inhibitors respectively.
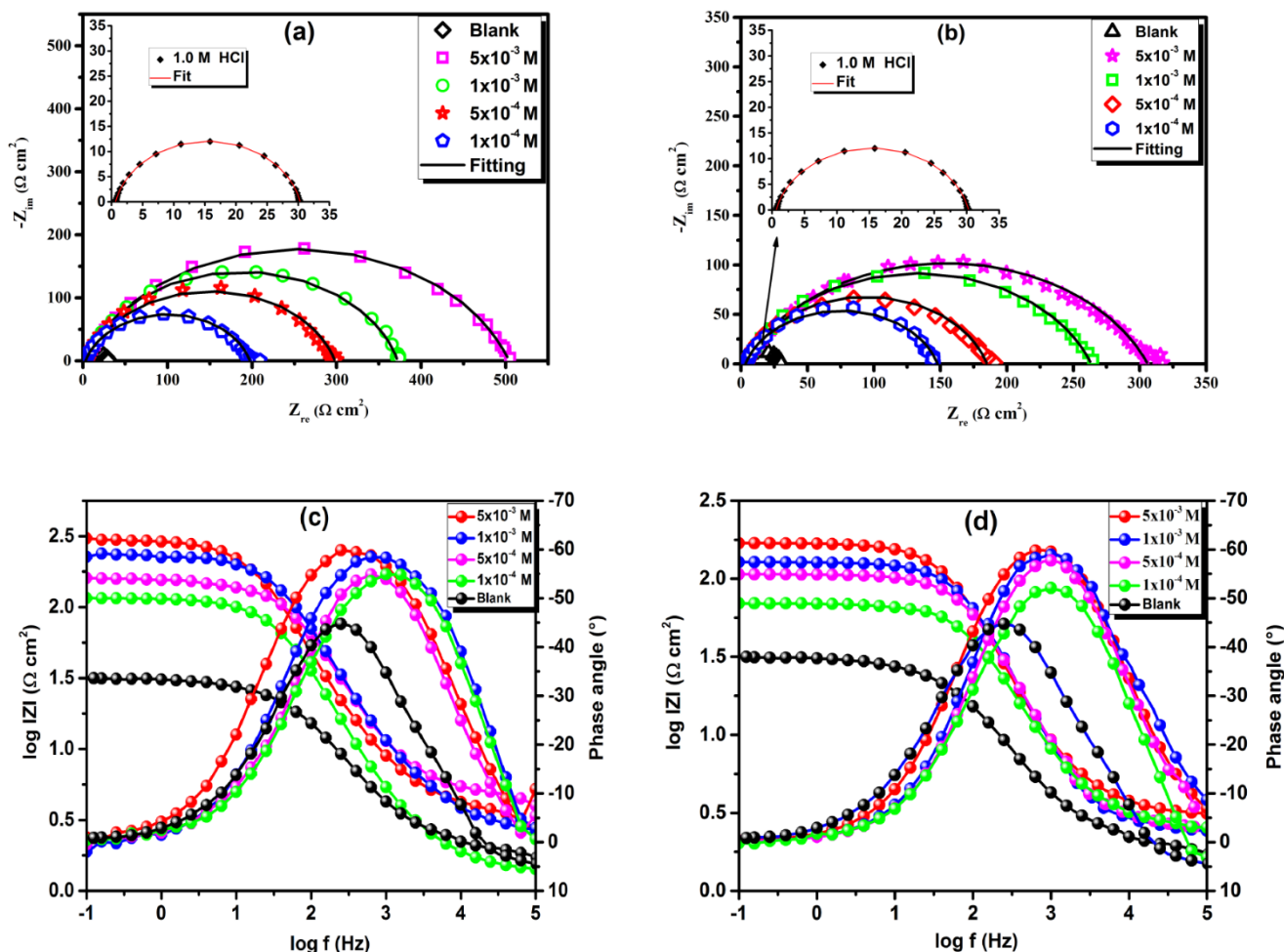
Figure 5. Nyquist and Bode diagrams of mild steel in 1.0 M HCl with and without various concentrations: (a, c) MMBH and (b, d) CBMP.

The values extracted from the figures R_p, C_{dl}, CPE, n, R_s and η_{EIS} are given in Table 6. The obtained plots of impedance are showing a capacitive loop that increases in size with increasing inhibitor concentrations, that is attributable to the charge transfer process. Therefore, R_p values with corrosion resistance significance have been achieved by fitting the EIS diagrams with the equivalent circuit shown in the insert Fig. 6.
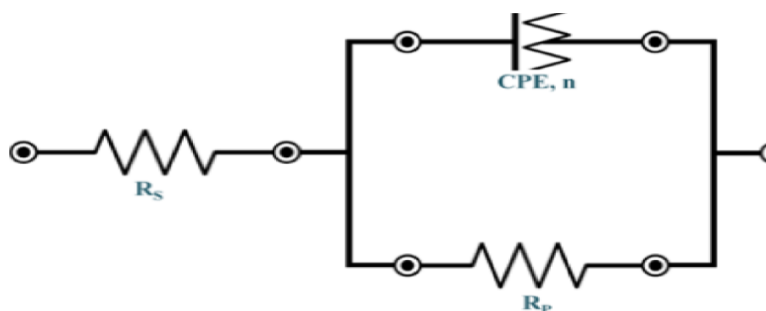
Figure 6. Equivalent circuit model applied to fit and simulate the impedance data

For the simulation of the EIS, the equivalent circuit used made up of a solution resistance R_s (uncompensated resistance in Ohm cm^2); a constant phase element (CPE); interfacial capacitance and R_p (Ohm cm^2) [34]. With the addition of the two inhibitors, the polarization resistance values were continuously improved with the increase in the concentration of the tested organic compounds. In contrast, C_{dl} values showed a significant decrease. As a result, the interface between the electrolyte and the metal is modified through the strong increase in the thickness of the electrical double layer as a result of the adsorption of a large number of molecules on the surface of the MS [35]. Also, the Bode and phase angle diagrams were used for further evaluation of MS corrosion resistance. The general idea is that if the phase angle becomes more negative, this assumes a capacitive electrochemical character [36]. However, increasingly, phase-angle values reach 65° relative to the blank, suggesting for both inhibitors to be markedly effective against MS corrosion [37].

Table 6. Electrochemical parameter values estimated according to EIS curves of MS in HCl solution in the presence and absence of several concentrations of MMBH and CBMP at 303 K.

| Inhibitor	Concentration (M)	R_p ($\Omega\ cm^2$)	n	$Q \times 10^{-4}$ ($S^n\Omega^{-1}cm^{-2}$)	C_{dl} ($\mu F/cm^2$)	η_{EIS} (%)	θ
Blank	1.0	29 ± 1.5	0.89 ± 0.005	1.7610 ± 0.0025	91	-	-
	5×10^{-3}	500 ± 1.6	0.79 ± 0.005	0.3872 ± 0.0024	13	94	0.94
MMBH	1×10^{-3}	368 ± 1.2	0.78 ± 0.007	0.5032 ± 0.0059	16	92	0.92
	5×10^{-4}	293 ± 1.0	0.81 ± 0.006	0.6348 ± 0.0066	24	89	0.99
	1×10^{-4}	194 ± 0.9	0.77 ± 0.009	1.1290 ± 0.0031	36	84	0.84
	5×10^{-3}	302 ± 0.5	0.77 ± 0.007	0.6381 ± 0.0091	19	90	0.90
CBMP	1×10^{-3}	260 ± 1.1	0.78 ± 0.002	0.7878 ± 0.0083	26	88	0.88
	5×10^{-4}	181 ± 1.7	0.80 ± 0.009	0.9808 ± 0.0024	35	83	0.83
	1×10^{-4}	144 ± 1.1	0.76 ± 0.006	1.4818 ± 0.0020	44	79	0.79

3.3.2. Immersion time effect

Due to the awareness of the influence of immersion time as an important part of the inhibitor adsorption process on the MS surface and having a considerable impact on the inhibitory efficacy, EIS results showing MMBH curves relative to immersion time are represented in Fig. 7. The improvement in inhibitory efficacy and the estimated parameters are grouped in Table 7. For this purpose, the electrochemical impedance analyses are conducted in 1.0 M HCl, without and in the presence of the investigated molecule, following different immersion times (30 min, 6 h, 12 h, and 24 h).

Table 7. EIS parameters for mild steel in the absence and presence of MMBH *vs.* immersion time.

Inhibitor	Time (h)	R_p ($\Omega\,cm^2$)	n	$Q \times 10^{-4}$ ($S^n\Omega^{-1}cm^{-2}$)	C_{dl} ($\mu F/cm^2$)	η_{EIS} (%)	θ
Blank	0.5	29 ± 1.5	0.89 ± 0.005	1.7610 ± 0.0025	92	-	-
	6	23 ± 2.5	0.84 ± 0.007	2.5114 ± 0.0037	94	-	-
	12	18 ± 1.7	0.83 ± 0.004	2.9866 ± 0.0084	102	-	-
	24	12 ± 2.9	0.88 ± 0.003	3.0891 ± 0.0031	144	-	-
MMBH	0.5	500 ± 1.6	0.79 ± 0.005	0.3872 ± 0.0024	13	94	0.94
	6	419 ± 1.5	0.80 ± 0.013	0.4585 ± 0.0020	17	94	0.94
	12	350 ± 1.4	0.78 ± 0.002	0.7489 ± 0.0041	26	94	0.94
	24	326 ± 1.8	0.79 ± 0.007	0.1386 ± 0.0033	33	96	0.96

According to Fig. 7, we notice the appearance of a single capacitive loop after all the tested immersion times. The polarization resistance of MS in the presence of 5×10^{-3} M of MMBH reduces as the immersion time increases. As shown in Table 7, it can be seen that the corrosion inhibiting effects of MMBH is nearly dependable with increasing immersion time. The reason behind this is the number of unoccupied sites [25–27]. Thus, when the steel is exposed for the first time in the inhibited environment, no sites are occupied. Therefore, the attractive forces between the surface vaccination and the free electrons of the heteroatom molecules will occur, which helps to improve the efficiency during the first 30 minutes of immersion.
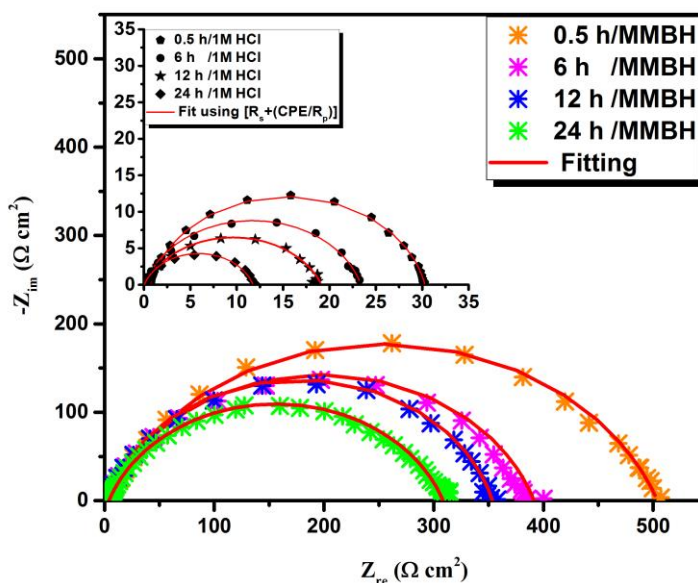
Figure 5. EIS curves of MS substrate immersed in 1.0 M HCl solution without and with 5×10^{-3} M of MMBH at varied times

3.4. Adsorption isotherm

One of the most typical processes for inhibitory molecules is adsorption. Due to this, it is possible to confirm the adsorption behavior of the molecule under examination by adapting the obtained results to many known adsorption isotherms [38]. Along with the Langmuir adsorption isotherm model, three other different types of adsorption isotherms, including Freundlich, Frumkin and Flory-Huggins, were evaluated. In this study, of the previously mentioned model of isotherms, it should be noted that the best fit was accomplished from the Langmuir model. In this case, the result is based on the value of the linear regression coefficient R^2, which is adjacent to 1. Moreover, the Langmuir isotherm describes the adsorption of the studied inhibitors onto the MS surface on the assumption of equivalent surface coverage, both homogeneous surface and active sites. Standard functionalities are given as follows [38]:

$$\frac{C}{\theta} = \frac{1}{K_{ads}} + C \qquad (9)$$

In which C signifies the inhibitor concentration, K_{ads} means a constant of adsorption equilibrium while θ denotes the area coverage. Free adsorption energies (ΔG^0_{ads}) are estimated using the equation 11 [39]:

$$K_{ads} = \frac{1}{55.5} \times exp\left(-\frac{\Delta G^O_{ads}}{RT}\right) \qquad (10)$$

In the above equation, as 55.5 points to the water molar concentration measured in mol L^{-1}, where T indicates the temperature of the aqueous solution and R is known as the universal gas constant. The adsorption parameters ΔH°_{ads} and ΔS°_{ads} on the MS surface is computed according to the next relationship:

$$\Delta G^{\circ}_{ads} = \Delta H^{\circ}_{ads} - T\Delta S^{\circ}_{ads} \qquad (11)$$

To illustrate this, we have drawn C/θ as a function of C in Fig. 8 (a). The thermodynamic parameters estimated from Langmuir's plot are tabulated in Table 8. This later confirms that the studied inhibitors are strongly adsorbed to the surface of the metal from high K_{ads} values [40–43].

Table 8. Thermodynamic parameters of MS corrosion in the presence of MMBH and CBMP in 1.0 M HCl obtained by Langmuir isotherm model.

Inhibitor	Temperature (K)	K_{ads} (M^{-1})	R^2	ΔG^0_{ads} (kJ/mol)	ΔH_a (kJ mol^{-1})	ΔS_a (J mol^{-1} K^{-1})
CBMP	303	47042	0.999	-37.20	-	-
MMBH	303	32570	0.999	-39.42		
	313	28920	0.999	-38.50	-72.14	-10.73

| | 323 | 34869 | 0.999 | -37.16 | |
| | 333 | 23143 | 0.999 | -36.27 | |
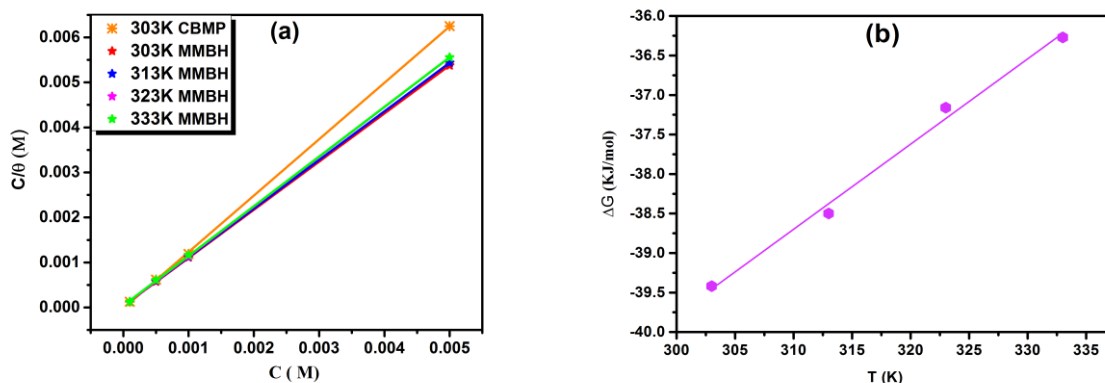
Figure 8. Langmuir adsorption isotherm plots (a), and regularity of the standard Gibbs free energy ΔG of MMBH vs. the temperature (b), on MS in 1.0 M HCl in different temperatures.

Findings from ΔG_{ads}° validated that both compounds adsorbed on the MS surface by a combination of chemical and physical interactions [55]. The setting of negative values ΔH_{ads}° and ΔS_{ads}° entails an exothermic adsorption of the inhibitor on MS sustained with reduced entropy [39]. Results also confirm the mixed type of adsorption.

3.5. SEM/EDX studies

A scanning electron microscopy analysis aimed at the assessment of the morphology of the MS surface to see if inhibition was due to a film of organic molecule formed on the surface, was used. The surface morphologies of the surveyed MS using SEM images are shown in Fig. 9 (a) and (b). The samples have been treated for 24 hours in a non-inhibited solution and those inhibited with the MMBH compound at a concentration of $5×10^{-3}$ M. The clearest thing that can be seen in Fig. 9 (a) is that the surface is corroded and contains internal corrosion damage, which is probably due to rapid corrosion attack in an aggressive environment.
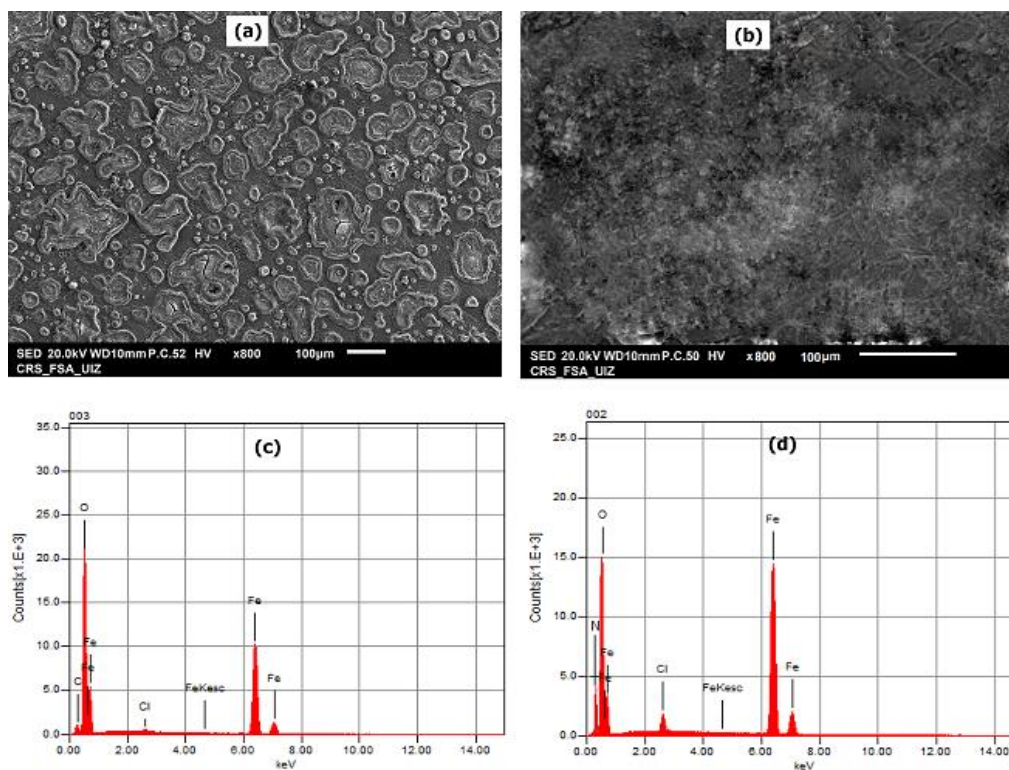
Figure 9. SEM and EDX images of MS surface, after 24 hrs immersion in 1.0 M HCl solution in the absence and the presence of 5×10^{-3} M of MMBH

However, the surface was smoother in the presence of inhibitor, as shown in Fig. 9 (b). The protection mechanism was understood by EDX analyses of the steel surface after 24 hours of immersion in HCl. The presence of peaks corresponding to oxygen, carbon and iron in the latter medium was detected by EDX analysis on the MS substrate before the addition of inhibitor (Fig.9 (c)). When the spectrum of the sample in the presence of MMBH is compared with the blank spectrum (Fig.9 (d)), it is clear that the chlorine and oxygen peak decreases on the EDX spectra in the presence of an inhibitor. These findings support that the MMBH compound inhibits the corrosion of the steel by forming a layer that limits the access of electrolytes to the surface. This happens through an adsorption mechanism in which the presence of nitrogen, aromatic rings and oxygen act as a significant factor in fixing the molecule to the surface, confirming the effectiveness of hydrazone derivatives in general, and also thanks to the presence of the donor groups which improves the effectiveness of MMBH in particular [44].

4. CONCLUSION

(E)-N'-(4-chlorobenzylidene)-2-(6-methoxynaphthalen-2-yl)propanehydrazide (CBMP) and ((E)-2-(6-methoxynaphthalen-2-yl)-N'-(4-methylbenzylidene) propanehydrazide(MMBH) are both synthesized and experimentally studied and tested as corrosion inhibitors in 1.0 M HCl. Overall, these study results show that due to the functional properties of hydrazones derivatives, the inhibitory power is approved. The main conclusions drawn from the results of this research are as follows:

- MNBH and MMBH acted as effective MS corrosion inhibitors in aqueous acidic conditions.
- Their polarization curves proved a mixed character of the inhibitors.
- The adsorption of studied compounds obeyed Langmuir's model and is done according to a combination of physical and chemical adsorption.
- Research into the influence of temperature on inhibitory efficacy suggests that it decreases with increasing temperature, confirming that the adsorption of molecules on the surface is by adsorption intermediate between physisorption and chemisorption.
- Moreover, the development of the protecting layer has been affirmed using SEM and EDX analysis.

To understand the link between the inhibitory efficacy of the two compounds and their molecular structure, an in-depth theoretical study is going to be detailed in a forthcoming article in which we will focus on the theoretical study of tested hydrazone derivatives.

CONFLICT OF INTEREST
"The authors of this manuscript have no conflict of interest to declare."

References

1. M. Hegazy, A. El-Tabei, A. Bedair, M. Sadeq, *RSC Advances*, 5 (2015) 64633–64650.
2. A. Popova, E. Sokolova, S. Raicheva, M. Christov, *Corrosion Science*, 45 (2003) 33–58.
3. W. Li, Q. He, S. Zhang, C. Pei, B. Hou, *Journal of Applied Electrochemistry*, 38 (2008) 289–295.
4. M. Deyab, *Desalination*, 439 (2018) 73–79.
5. F. Bentiss, C. Jama, B. Mernari, H. El Attari, L. El Kadi, M. Lebrini, M. Traisnel, M. Lagrenée, *Corrosion Science*, 51 (2009) 1628–1635.
6. I. Glasgow, A. Rostron, G. Thomson, *Corrosion Science*, 6 (1966) 469–482.
7. N. Soltani, M. Behpour, E. Oguzie, M. Mahluji, M. Ghasemzadeh, *RSC Advances*, 5 (2015) 11145–11162.
8. P. Singh, V. Srivastava, M. Quraishi, *Journal of Molecular Liquids*, 216 (2016) 164–173.
9. Y. Zhang, Y. Cheng, F. Ma, K. Cao, *International Journal of Electrochemical Science*, 14 (2019) 999–1008.
10. F. Bentiss, M. Outirite, M. Traisnel, H. Vezin, M. Lagrenée, B. Hammouti, S.S. Al-Deyab, C. Jama, *International Journal of Electrochemical Science*, 7 (2012) 1699–1723.
11. M.A. Ameer, A.M. Fekry, A. Othman, *International Journal of Electrochemical Science*, 9 (2014) 1964–1985.
12. G. Khan, W.J. Basirun, A.B.B.M. Badry, S.N. Kazi, P. Ahmed, S.M. Ahmed, G.M. Khan, *International Journal of Electrochemical Science*, 13 (2018) 12420–12436.
13. X. Zhang, B. Tan, *International Journal of Electrochemical Science*, 13 (2018) 11388–11404.

14. H. Lgaz, R. Salghi, I.H. Ali, *International Journal of Electrochemical Science*, 13 (2018) 250–264.
15. S. Rollas, S.G. Küçükgüzel, *Molecules*, 12 (2007) 1910–1939.
16. A.G. Al-Sehemi, A. Irfan, M. Alfaifi, A.M. Fouda, T.M. El-Gogary, D.A. Ibrahim, *Journal of King Saud University-Science*, 29 (2017) 311–319.
17. A. Almasirad, M. Tajik, D. Bakhtiari, A. Shafiee, M. Abdollahi, M.J. Zamani, R. Khorasani, H. Esmaily, *J Pharm Pharm Sci*, 8 (2005) 419–425.
18. H. Lgaz, S. Zehra, M.R. Albayati, K. Toumiat, Y. El Aoufir, A. Chaouiki, R. Salghi, I.H. Ali, M.I. Khan, I.-M. Chung, S.K. Mohamed, *International Journal of Electrochemical Science*, 14 (2019) 6667–6681.
19. H. Lgaz, A. Chaouiki, M.R. Albayati, R. Salghi, Y. El Aoufir, I.H. Ali, M.I. Khan, S.K. Mohamed, I.-M. Chung, *Research on Chemical Intermediates*, 45 (2019) 2269–2286.
20. H. Lgaz, I.-M. Chung, M.R. Albayati, A. Chaouiki, R. Salghi, S.K. Mohamed, *Arabian Journal of Chemistry*, 13 (2020) 2934–2954.
21. A. Chaouiki, M. Chafiq, H. Lgaz, M.R. Al-Hadeethi, I.H. Ali, S. Masroor, I.-M. Chung, *Coatings*, 10 (2020) 640.
22. J. Scully, R. Baboian, ASTM Phila PA (1995).
23. P. American Society for Testing and Materials (Filadelfia, ASTM, (2004).
24. F. Tezcan, G. Yerlikaya, A. Mahmood, G. Kardaş, *Journal of Molecular Liquids*, 269 (2018) 398–406.
25. H. Lgaz, R. Salghi, S. Jodeh, B. Hammouti, *Journal of Molecular Liquids*, 225 (2017) 271–280.
26. A. Bousskri, A. Anejjar, M. Messali, R. Salghi, O. Benali, Y. Karzazi, S. Jodeh, M. Zougagh, E.E. Ebenso, B. Hammouti, *Journal of Molecular Liquids*, 211 (2015) 1000–1008.
27. I. Obot, N. Obi-Egbedi, E. Ebenso, A. Afolabi, E. Oguzie, *Research on Chemical Intermediates*, 39 (2013) 1927–1948.
28. A.K. Singh, E.E. Ebenso, M. Quraishi, *Int. J. Electrochem. Sci*, 7 (2012) 2320.
29. S.K. Shukla, M. Quraishi, *Corrosion Science*, 51 (2009) 1990–1997.
30. F. Bentiss, F. Gassama, D. Barbry, L. Gengembre, H. Vezin, M. Lagrenée, M. Traisnel, *Applied Surface Science*, 252 (2006) 2684–2691.
31. M. Chakravarthy, K. Mohana, C.P. Kumar, *International Journal of Industrial Chemistry*, 5 (2014) 19.
32. W. Chen, S. Hong, B. Xiang, H. Luo, M. Li, N. Li, *Corrosion Engineering, Science and Technology*, 48 (2013) 98–107.
33. M. Faustin, A. Maciuk, P. Salvin, C. Roos, M. Lebrini, *Corrosion Science*, 92 (2015) 287–300.
34. M. Behpour, S. Ghoreishi, N. Mohammadi, N. Soltani, M. Salavati-Niasari, *Corrosion Science*, 52 (2010) 4046–4057.
35. H. Lgaz, R. Salghi, K.S. Bhat, A. Chaouiki, S. Jodeh, *Journal of Molecular Liquids*, 244 (2017) 154–168.
36. M. Mahdavian, M. Attar, *Corrosion Science*, 48 (2006) 4152–4157.
37. L. Larabi, Y. Harek, M. Traisnel, A. Mansri, *Journal of Applied Electrochemistry*, 34 (2004) 833–839.
38. M.E. Belghiti, S. Tighadouini, Y. Karzazi, A. Dafali, B. Hammouti, S. Radi, R. Solmaz, *J Mater Environ Sci 2016a*, 7 (2007) 337–346.
39. S.A. Umoren, U.M. Eduok, M.M. Solomon, A.P. Udoh, *Arabian Journal of Chemistry*, 9 (2016) S209–S224.
40. X. Li, S. Deng, T. Lin, X. Xie, G. Du, *Corrosion Science*, 118 (2017) 202–216.
41. J. Aljourani, K. Raeissi, M. Golozar, *Corrosion Science*, 51 (2009) 1836–1843.
42. D.M. Gurudatt, K.N. Mohana, *Industrial & Engineering Chemistry Research*, 53 (2014) 2092–2105.
43. M. Mahdavian, S. Ashhari, *Electrochimica Acta*, 55 (2010) 1720–1724.

44. M. El Azzouzi, A. Aouniti, S. Tighadouin, H. Elmsellem, S. Radi, B. Hammouti, A. El Assyry, F. Bentiss, A. Zarrouk, *Journal of Molecular Liquids*, 221 (2016) 633–641.